

advances.sciencemag.org/cgi/content/full/6/47/eabd7697/DC1

Supplementary Materials for

Gating by ionic strength and safety check by cyclic-di-AMP in the ABC transporter OpuA

Hendrik R. Sikkema, Marco van den Noort, Jan Rheinberger, Marijn de Boer, Sabrina T. Krepel,
Gea K. Schuurman-Wolters, Cristina Paulino*, Bert Poolman*

*Corresponding author. Email: b.poolman@rug.nl (B.P.); c.paulino@rug.nl (C.P.)

Published 18 November 2020, *Sci. Adv.* **6**, eabd7697 (2020)
DOI: [10.1126/sciadv.abd7697](https://doi.org/10.1126/sciadv.abd7697)

This PDF file includes:

Figs. S1 to S6
Table S1

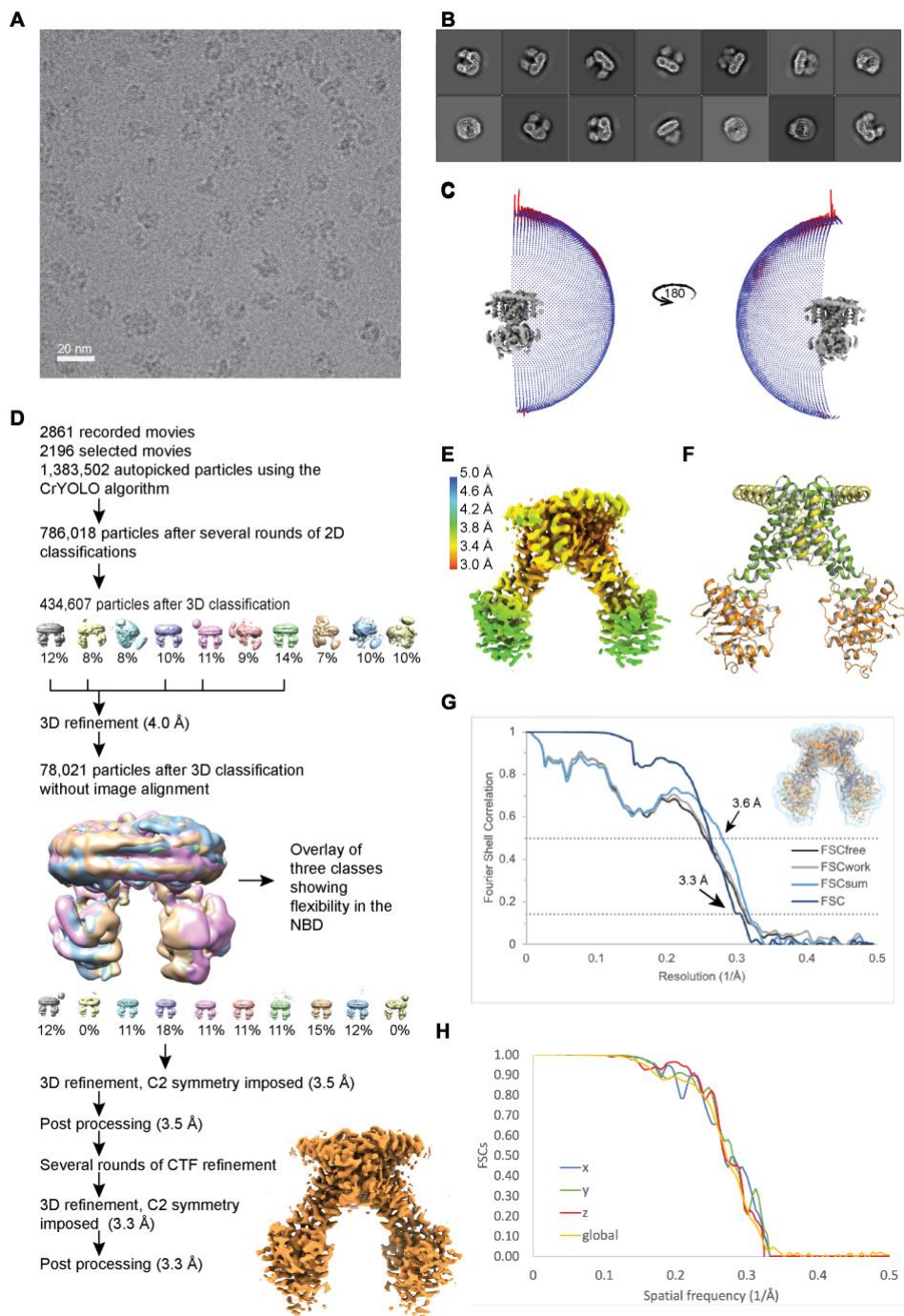


Fig. S1. Processing of *apo* inward-facing conformation of OpuA. (A) Zoom-in of a representative cryo-EM image. (B) Representative 2D class averages. (C) Angular distribution plot of the final C2 symmetrized 3D reconstruction. (D) Image processing workflow. (E) Local resolution estimation of the final reconstruction by Relion. (F) Final model, see Table S1 for validation parameters. (G) FSC plot used for resolution estimation and model validation. The gold-standard FSC plot between two separately refined half-maps is shown in dark blue and indicates a final resolution of 3.3 Å. The FSC model validation curves for FSCsum, FSCwork and FSCfree, as described in material and methods, are shown in light blue, light grey and dark grey, respectively. A thumbnail of the mask used for FSC calculation overlaid on the map is shown in the upper right corner. Dashed lines indicate the FSC thresholds used for FSC of 0.143 and for FSCsum of 0.5. (H) Estimation of anisotropy by the 3DFSC webserver. The calculated sphericity was 0.969. FSC curves along x, y and z axes are shown in blue, green and red, respectively. The global FSC is shown in yellow.

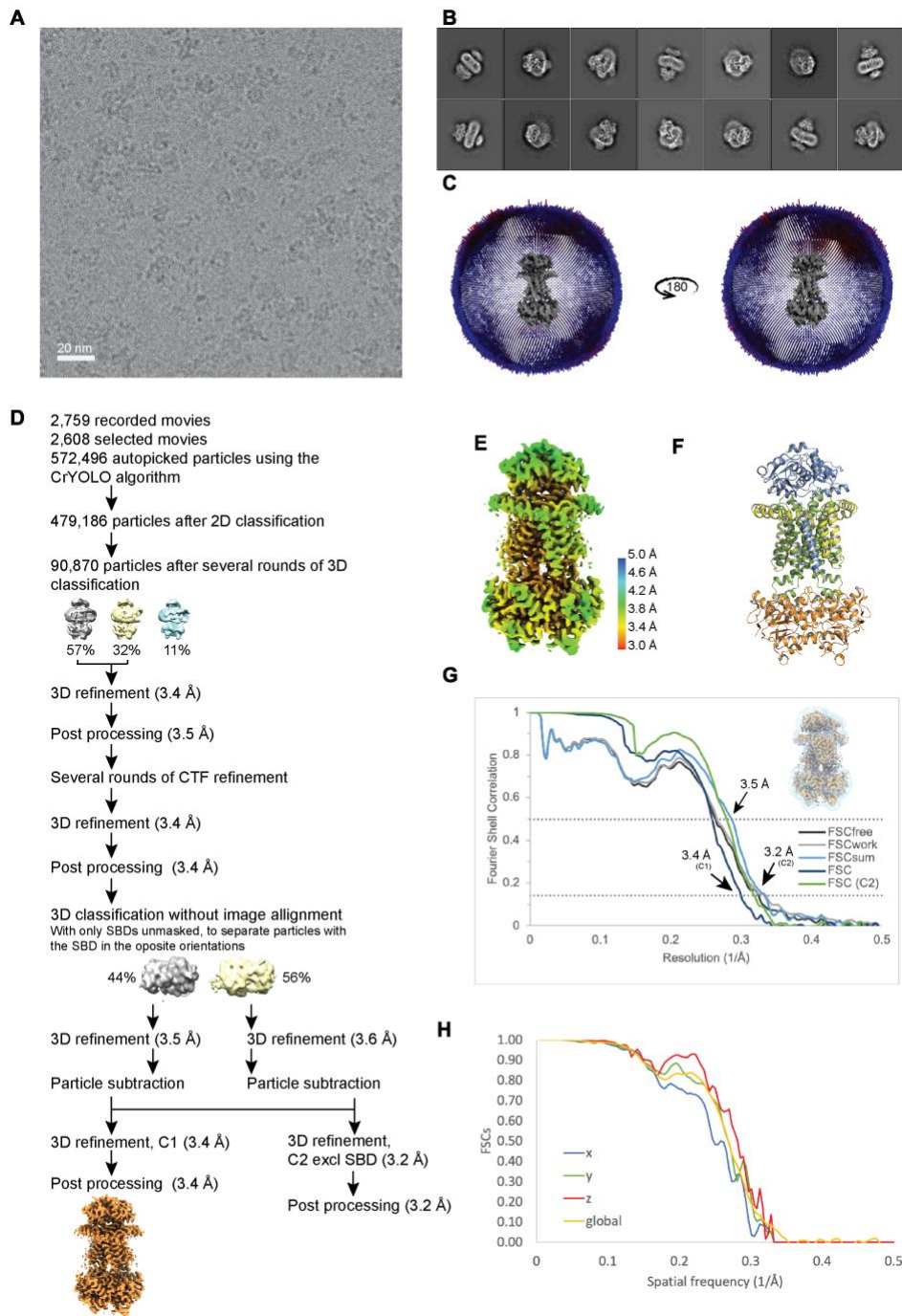


Fig. S2. Processing of OpuA (E190Q) structure in occluded conformation. (A) Zoom-in of a representative cryo-EM image. (B) Representative 2D class averages. (C) Angular distribution plot of the final 3D reconstruction. (D) Image processing workflow. (E) Local resolution estimation of the final reconstruction by Relion. (F) Final model, see Table S1 for validation parameters. (G) FSC plot used for resolution estimation and model validation. The gold-standard FSC plot between two separately refined half-maps is shown in dark blue and indicates a final resolution of 3.4 Å for C1, and the same FSC for the C2 symmetrized map is shown in green (3.2 Å). The FSC model validation curves for FSCsum, FSCwork and FSCfree, as described in material and methods, are shown in light blue, light grey and dark grey, respectively. A thumbnail of the mask used for FSC calculation overlaid on the map is shown in the upper right corner. Dashed lines indicate the FSC thresholds used for FSC of 0.143 and for FSCsum of 0.5. (H) Estimation of anisotropy by the 3DFSC webserver. The calculated sphericity was 0.969. FSC curves along x,y and z axes are shown in blue, green and red, respectively. The global FSC is shown in yellow.

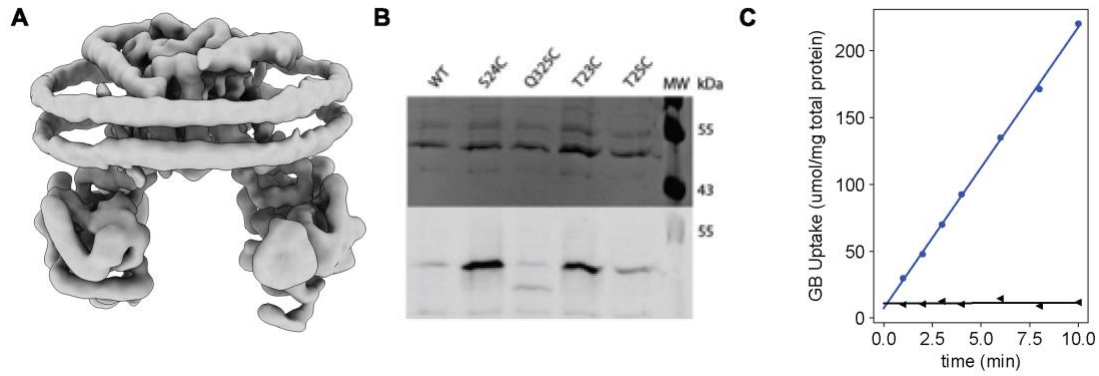


Fig. S3. MSP wrapping and scaffold domain

(A) Cryo-EM reconstruction of substrate-free, *apo* OpuA, refined without a mask, showing clear densities for the two MSP1D1 helices wrapped around OpuA, forming the nanodisc assembly. (B) Coomassie brilliant blue-stained (top) and *in gel* fluorescence (bottom) of an SDS-PAA gel showing wildtype OpuA, OpuA-scaffold mutants S24C, T23C and T25C, and the control NBD mutant Q325C, after *in vivo* labeling with membrane-impermeable fluorescein-5-maleimide (see Methods). Cys-23 and Cys-24 are accessible on the external surface of the cell for labeling by the membrane-impermeable fluorescein-5-maleimide, which is in agreement with the location of the amphipatic helices of the scaffold domain in the cryo-EM structures of OpuA. Cys-25 and Cys325 (inside of cell) show background labeling comparable to the Cys-less wildtype OpuA. (C) *In vivo* glycine betaine (GB) uptake by wildtype OpuA (blue) and OpuA with the scaffold domain deleted (OpuA Δ SD) (black).

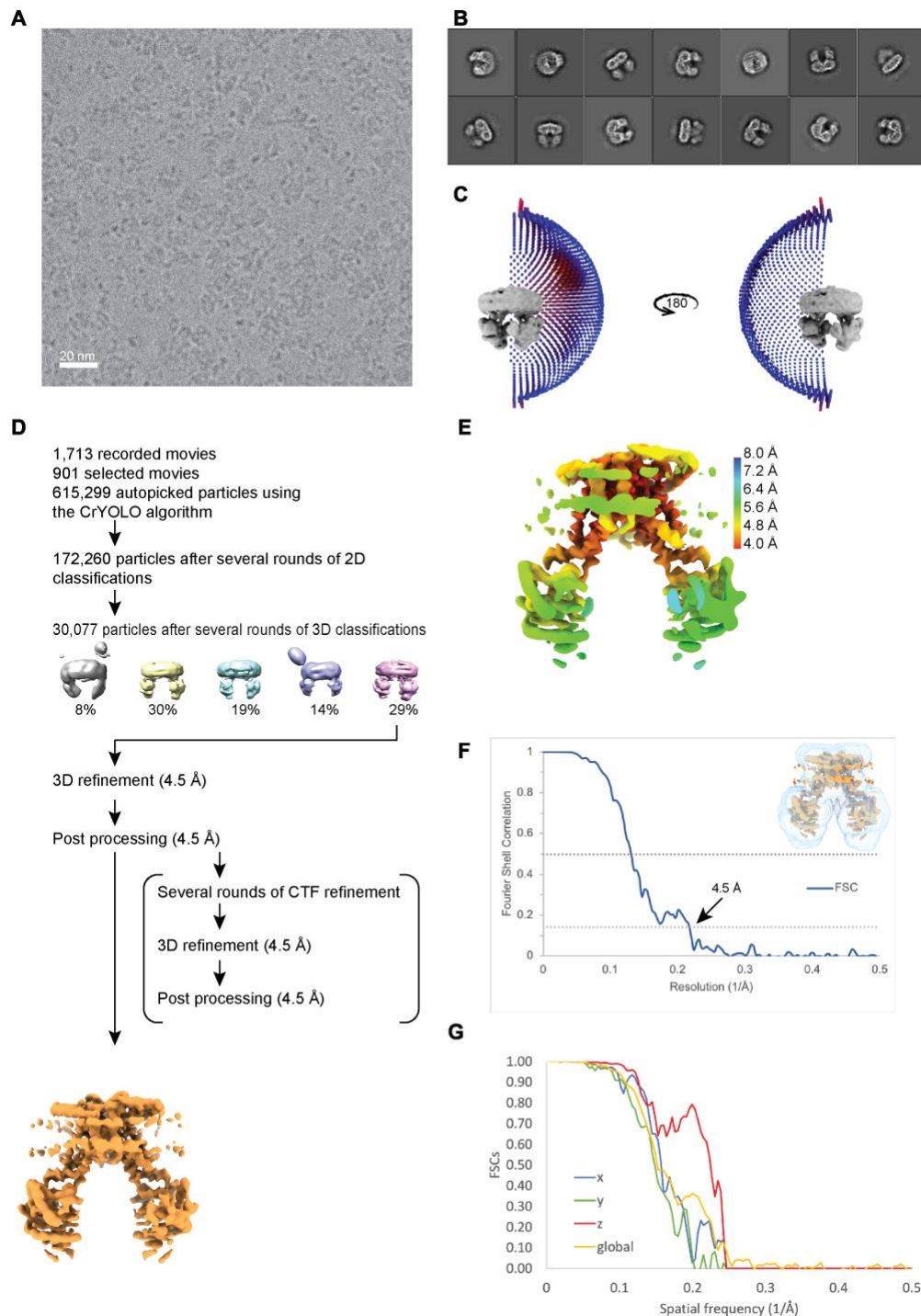


Fig. S4. Processing of OpuA structure in the presence of glycine betaine. (A) Zoom-in of a representative cryo-EM image. (B) Representative 2D class averages. (C) Angular distribution plot of the final C2 symmetrized 3D reconstruction. (D) Image processing workflow. (E) Local resolution estimation of the final reconstruction by Relion. (F) FSC plot used for resolution estimation. The gold-standard FSC plot between two separately refined half-maps is shown in blue and indicates a final resolution of 4.5 Å. A thumbnail of the mask used for FSC calculation overlaid on the map is shown in the upper right corner. Dashed lines indicate the FSC thresholds used for FSC of 0.143 and for FSCsum of 0.5. (G) Estimation of anisotropy by the 3DFSC webserver. The calculated sphericity was 0.805. FSC curves along x,y and z axes are shown in blue, green and red, respectively. The global FSC is shown in yellow.

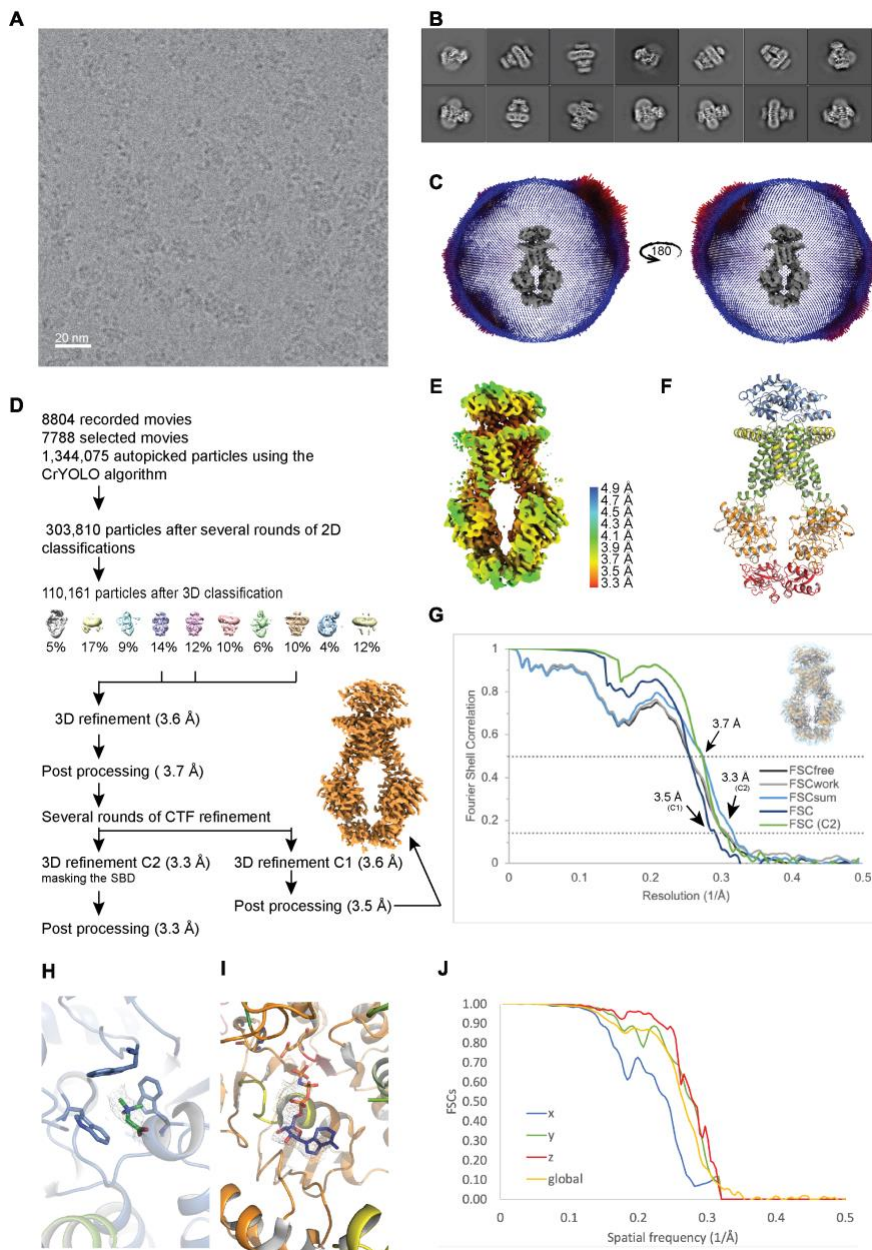


Fig. S5. Processing of OpuA structure in the presence of glycine betaine, cyclic-di-AMP and AMP-PNP. (A) Zoom-in of a representative cryo-EM image. (B) Representative 2D class averages. (C) Angular distribution plot of the final 3D reconstruction. (D) Image processing workflow. (E) Local resolution estimation of the final reconstruction by Relion. (F) Final model, see Table S1 for validation parameters. (G) FSC plot used for resolution estimation and model validation. The gold-standard FSC plot between two separately refined half-maps is shown in blue and indicates a final resolution of 3.5 Å for C1, and the same FSC for the C2 symmetrized map is shown in green (3.3 Å). The FSC model validation curves for FSCsum, FSCwork and FSCfree, as described in material and methods, are shown in light blue, light grey and dark grey, respectively. A thumbnail of the mask used for FSC calculation overlaid on the map is shown in the upper right corner. Dashed lines indicate the FSC thresholds used for FSC of 0.143 and for FSCsum of 0.5. (H) Binding site of glycine betaine in the SBD, and (I) binding site of AMP-PNP in the NBD of OpuA in the presence of glycine betaine, cyclic-di-AMP and AMP-PNP. Density around ligands are shown as mesh at 6σ . (J) Estimation of anisotropy by the 3DFSC webserver. The calculated sphericity was 0.958. FSC curves along x,y and z axes are shown in blue, green and red, respectively. The global FSC is shown in yellow.

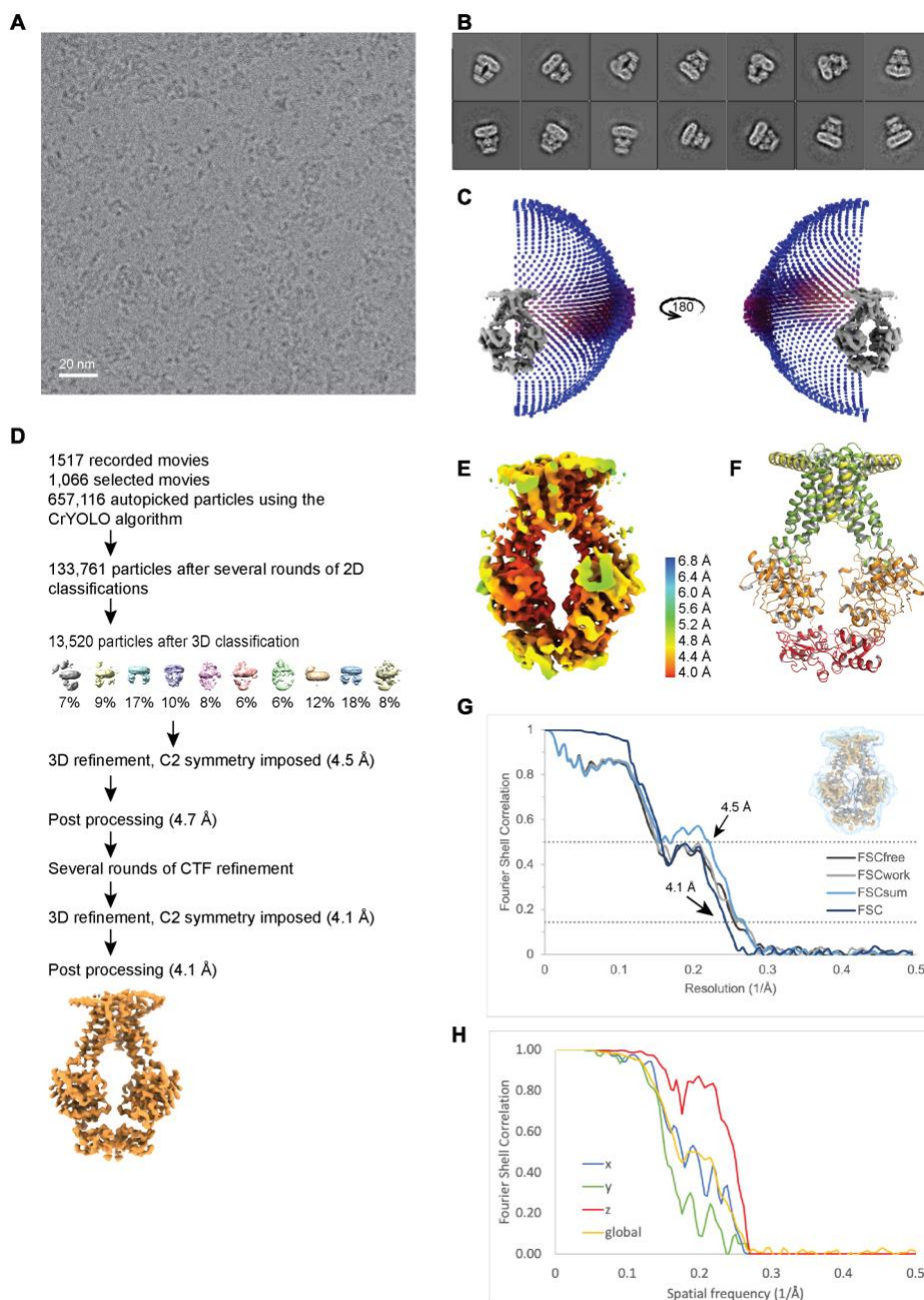


Fig. S6. Processing of OpuA structure in the presence of cyclic-di-AMP. (A) Zoom-in of a representative cryo-EM image. (B) Representative 2D class averages. (C) Angular distribution plot of the final C2 symmetrized 3D reconstruction, with C2 symmetry imposed. (D) Image processing workflow. (E) Local resolution estimation of the final reconstruction by Relion. (F) Final model, see Table S1 for validation parameters. (G) FSC plot used for resolution estimation and model validation. The gold-standard FSC plot between two separately refined half-maps is shown in blue and indicates a final resolution of 4.1 Å. The FSC model validation curves for FSCsum, FSCwork and FSCfree, as described in material and methods, are shown in light blue, light grey and dark grey, respectively. A thumbnail of the mask used for FSC calculation overlaid on the map is shown in the upper right corner. Dashed lines indicate the FSC thresholds used for FSC of 0.143 and for FSCsum of 0.5. (H) Estimation of anisotropy by the 3DFSC webserver. The calculated sphericity was 0.766. FSC curves along x,y and z axes are shown in blue, green and red, respectively. The global FSC is shown in yellow.

Table S1. Cryo-EM data collection, refinement and validation statistics

	OpuA (apo)	OpuA (E190Q) – Glycine betaine, ATP	OpuA – glycine betaine	OpuA – glycine betaine, cyclic-di-AMP, AMP-PNP	OpuA – cyclic-di-AMP
<i>Data collection and processing</i>					
Magnification	49,407	49,407	49,407	49,407	49,407
Voltage (kV)	200	200	200	200	200
Electron exposure (e ⁻ /Å ²)	53	53	53	53	53
Defocus range (µm)	0.5-2	0.5-2	0.5-2	0.5-2	0.5-2
Pixel size (Å)	1.012	1.012	1.012	1.012	1.012
Symmetry imposed	C2	C1 (C2)	C2	C1 (C2)	C2
Initial particle images (no.)	1,383,502	572,496	615,299	1,344,075	657,116
Final particle images (no.)	434,607	90,870	30,077	110,161	13,520
Map resolution (Å)	3.3	3.4 (3.2)	4.5	3.5 (3.3)	4.1
Fsc threshold	0.143	0.143	0.143	0.143	0.143
Map local resolution range (Å)	5.5 - 3.2	5.0 - 3.3	9.0 - 4.1	4.6 - 3.4	7.2 - 4.1
<i>Refinement</i>					
Initial model used	-	-	-	-	-
Model resolution (Å) (0.5 fsc threshold)	3.6	3.5	-	3.7	4.5
Model resolution range (Å)	15 – 3.3	15 – 3.4	-	15 – 3.5	15 – 4.1
Map sharpening b factor (Å ²)	-117.28	-88.6437	-141.293	-98.936	-126.983
Model composition					
Nonhydrogen atoms	8170	10562	-	12127	10062
Protein residues	1064	1361	-	1562	1308
Ligands	-	ATP:2,BET:1	-	ANP:2, BET:1, 2BA:1	2BA:1
B factors (Å ²)					
Protein	2.53/71.69/29.63	33.63/63.00/43.08	-	25.42/76.67/46.80	30.00/143.81/98.07
Ligand	-	37.87/38.90/38.37	-	50.16/58.81/55.08	93.00/93.00/93.00
R.m.s. Deviations					
Bond lengths (Å)	0.008	0.006	-	0.009	0.006
Bond angles (°)	0.606	0.741	-	0.989	0.981
Validation					
Molprobrity score	2.14	1.73	-	2.13	2.25
Clashscore	13.24	8.73	-	14.02	16.11
Poor rotamers (%)	0.11	0.79	-	0.23	0.36
Ramachandran plot					
Favoured (%)	91.48	96.21	-	92.38	90.35
Allowed (%)	8.52	3.79	-	7.62	9.65
Disallowed (%)	0	0	-	0	0